American Society of Hematology
2021 L Street NW, Suite 900,
Washington, DC 20036
Phone: 202-776-0544 | Fax 202-776-0545
editorial@hematology.org

Inducible CXCL12/CXCR4-dependent extramedullary hematopoietic niches in the adrenal gland

Tracking no: BLD-2023-020875R2

Frederica Schyrr (EPFL and University of Lausanne, Switzerland) Alejandro Alonso Calleja (EPFL and University of Lausanne, Switzerland) Anjali Vijaykumar (University and University Hospital Zurich, Switzerland) Jessica Sordet-Dessimoz (Ecole Polytechnique Fédérale de Lausanne (EPFL), Switzerland) Sandra Gebhard (Lausanne University Hospital (CHUV), Switzerland) Rita Sarkis (EPFL and University of Lausanne and University Hospital of lausanne, Switzerland) Charles Bataclan (University of Lausanne, Switzerland) Silvia Ferreira Lopes (University of Lausanne, Switzerland) Aurélien Oggier (EPFL, Switzerland) Laurence de Leval (Lausanne University Hospital, Switzerland) Cesar Nombela-Arrieta (University and University Hospital Zurich, Switzerland) Olaia Naveiras (University of Lausanne, Switzerland)

Abstract:
Adult hematopoietic Stem and Progenitor Cells (HSPCs) reside in the bone marrow hematopoietic niche, which regulates HSPC quiescence, self-renewal, and commitment in a demand-adapted manner. While the complex bone marrow niche is responsible for adult hematopoiesis, evidence exists for simpler, albeit functional and more accessible, extramedullary hematopoietic niches. Inspired by the anecdotal description of retroperitoneal hematopoietic masses occurring at higher frequency upon hormonal dysregulation within the adrenal gland, we hypothesized that the adult adrenal gland could be induced into a hematopoietic supportive environment in a systematic manner, thus revealing mechanisms underlying de novo niche formation in the adult. Here we show that upon splenectomy and hormonal stimulation, the adult adrenal gland of mice can be induced to recruit and host functional HSPCs, capable of serial transplantation, and that this phenomenon is associated with de novo formation of platelet-derived growth factor receptor α (PDGFRα) expressing stromal nodules. We further show in CXCL12-GFP reporter mice that adrenal glands contain a stromal population reminiscent of the CXCL12-Abundant Reticular (CAR) cells which compose the bone marrow HSPC niche. Mechanistically, HSPC homing to hormonally-induced adrenal glands was found dependent on the CXCR4/CXCL12 axis. Mirroring our findings in mice, we found reticular CXCL12+ cells co-expressing master niche-regulator FOXC1 in primary samples from human adrenal myelolipomas, a benign tumor composed of adipose and hematopoietic tissue. Our findings reignite long-standing questions regarding hormonal regulation of hematopoiesis and provide a novel model to facilitate the study of adult-specific inducible hematopoietic niches which may pave the way to therapeutic applications.

Conflict of interest: No COI declared

COI notes:

Preprint server: Yes; Biorxiv 10.1101/2023.03.15.531679

Author contributions and disclosures: ON and FS conceived the ideas and obtained funding for the project. FS performed all the experiments with the help of AAC, SFL and AO. FS, ON and AAC analyzed the results and wrote the manuscript. AV and CNA performed and analyzed all wholemount confocal microscopy imaging presented in this manuscript. RS, CB, JSD and LdL set up the immunostaining panel for human myelolipomas. SG assessed the myelolipoma images. FS and ON compiled the clinical data. First co-authorship was granted based on the final contribution to the completion of the project; FS developed the experimental pipelines and executed the experiments while AAC assisted during the experiments and was involved in the preparation of the manuscript, analysis of the data and finalization of the project.

Non-author contributions and disclosures: No;

Agreement to Share Publication-Related Data and Data Sharing Statement: Datasets will be deposited in Zenodo for the final version

Clinical trial registration information (if any):

Extramedullary Hematopoiesis in the Adrenal Gland of Mice and Humans

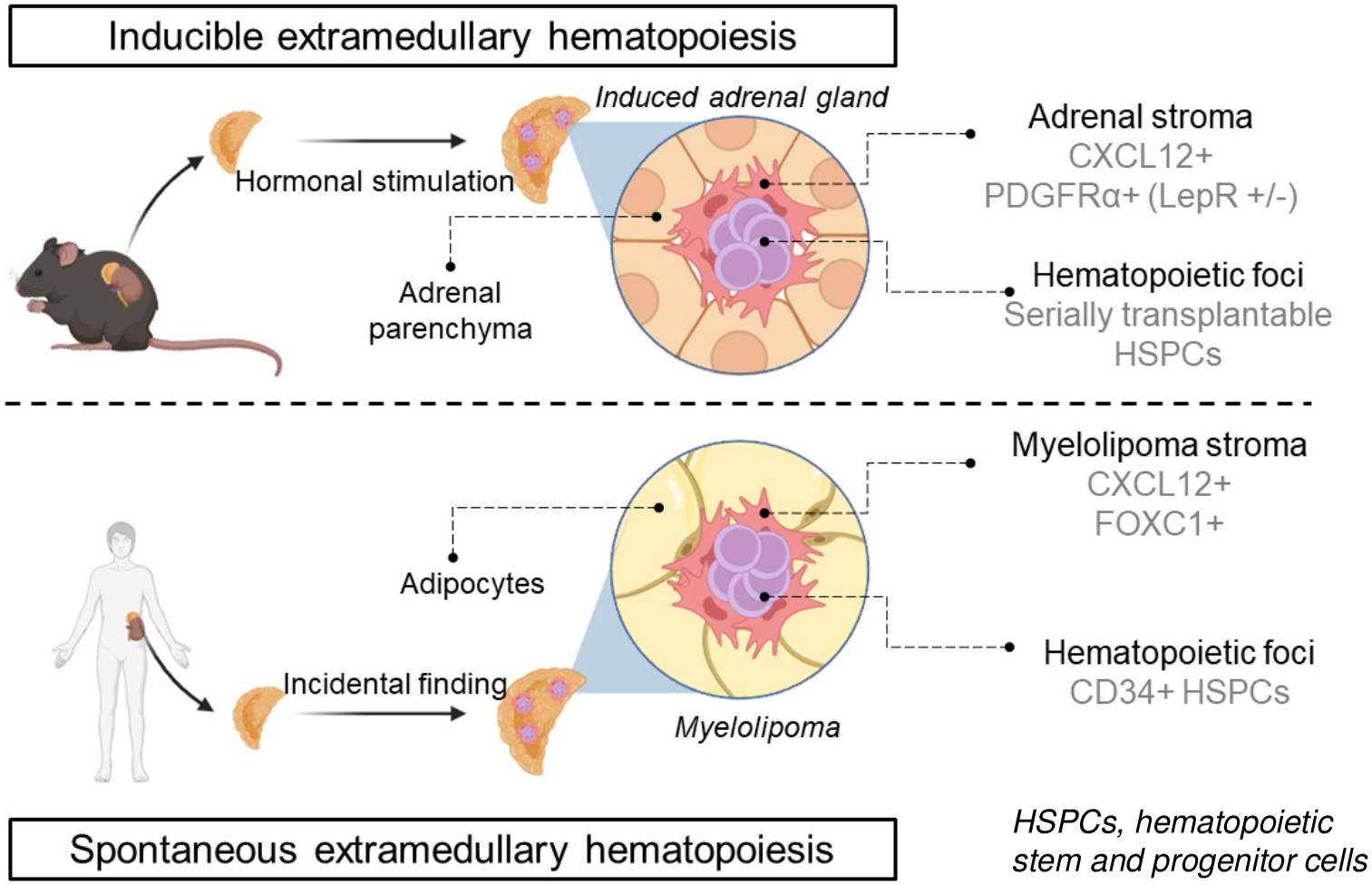

HSPCs, hematopoietic stem and progenitor cells

Conclusion: In mice, the adrenal glands can be induced to host HSPCs in niches containing CXCL12+ reticular cells. These cells are also found in human adrenal myelolipoma, a benign tumor composed of adipose and hematopoietic tissue.

*Schyrr et al. DOI: 10.xxxx/**blood**.2024xxxxxx*

***Blood* Visual Abstract**

Title: Inducible CXCL12/CXCR4-dependent extramedullary hematopoietic niches in the adrenal gland

Running title: Adrenal glands can host adult hematopoiesis.

Authors: Frédérica Schyrr[1,2]*, Alejandro Alonso-Calleja[1,2]*, Anjali Vijaykumar[3], Jessica Sordet-Dessimoz[4], Sandra Gebhard[5], Rita Sarkis[1,2], Charles Bataclan[1], Silvia Ferreira Lopes[1], Aurélien Oggier[2], Laurence de Leval[6], César Nombela-Arrieta[3], Olaia Naveiras[1,2, 7]

[1]Laboratory of Regenerative Hematopoiesis, Department of Biomedical Sciences, University of Lausanne, Switzerland

[2]Laboratory of Regenerative Hematopoiesis, Swiss Institute for Experimental Cancer Research (ISREC) & Institute of Bioengineering, École Polytechnique Fédérale de Lausanne (EPFL), Lausanne, Switzerland

[3]Hematology, University Hospital and University of Zurich, Zurich 8091, Switzerland

[4]Histology Core Facility, Ecole Polytechnique Fédérale de Lausanne, Lausanne, Switzerland.

[5] Anorexie boulimie Centre vaudois (abC), espace CHUV Service de psychiatrie de liaison, Département de psychiatrie, Lausanne University Hospital (CHUV) Lausanne, Switzerland.

[6] Institute of Pathology, Department of Laboratory Medicine and Pathology, Lausanne University Hospital and Lausanne University, Lausanne, Switzerland

[7] Hematology Service, Departments of Oncology and Laboratory Medicine, Lausanne University Hospital (CHUV) and University of Lausanne (UNIL), Lausanne, Switzerland

* These authors have contributed equally and share first co-authorship

Corresponding author information

- Full name: Olaia Naveiras
- Address: Department of Biomedical Sciences, University of Lausanne (UNIL), Switzerland, Rue du Bugnon 27. CH1011-Lausanne
- Telephone number: +41 21 692 54 37
- E-mail address: olaia.naveiras@unil.ch

Datasets will be deposited in Zenodo for the final version (assigned doi will be specified here)

- Word count: Main text: 3987 Abstract: 250. Reference count: 37

Figure count: main: 6; supplemental: 5. Table count: main: 1; supplemental tables: 2.

Category: HEMATOPOIESIS AND STEM CELLS

Key points

- The adrenal gland can be hormonally induced to host serially transplantable hematopoietic stem and progenitor cells in adult mice
- Adrenal extramedullary hematopoiesis is associated to the formation of PDGFRα+LepR+/- foci in mice and CXCL12+FOXC1+ stroma in humans

Abstract

Adult hematopoietic Stem and Progenitor Cells (HSPCs) reside in the bone marrow hematopoietic niche, which regulates HSPC quiescence, self-renewal, and commitment in a demand-adapted manner. While the complex bone marrow niche is responsible for adult hematopoiesis, evidence exists for simpler, albeit functional and more accessible, extramedullary hematopoietic niches. Inspired by the anecdotal description of retroperitoneal hematopoietic masses occurring at higher frequency upon hormonal dysregulation within the adrenal gland, we hypothesized that the adult adrenal gland could be induced into a hematopoietic supportive environment in a systematic manner, thus revealing mechanisms underlying de novo niche formation in the adult. Here we show that upon splenectomy and hormonal stimulation, the adult adrenal gland of mice can be induced to recruit and host functional HSPCs, capable of serial transplantation, and that this phenomenon is associated with de novo formation of platelet-derived growth factor receptor α (PDGFRα) expressing stromal nodules. We further show in CXCL12-GFP reporter mice that adrenal glands contain a stromal population reminiscent of the CXCL12-Abundant Reticular (CAR) cells which compose the bone marrow HSPC niche. Mechanistically, HSPC homing to hormonally-induced adrenal glands was found dependent on the CXCR4/CXCL12 axis. Mirroring our findings in mice, we found reticular CXCL12+ cells co-expressing master niche-regulator FOXC1 in primary samples from human adrenal myelolipomas, a benign tumor composed of

adipose and hematopoietic tissue. Our findings reignite long-standing questions regarding hormonal regulation of hematopoiesis and provide a novel model to facilitate the study of adult-specific inducible hematopoietic niches which may pave the way to therapeutic applications.

Introduction

While adult hematopoiesis takes place primarily in the bone marrow (BM), examples of adult hematopoiesis outside the bone cavity exist, grouped under the term extramedullary hematopoiesis (EMH). EMH can be classified in two groups [1] (i) EMH arising in fetal hematopoiesis sites, fundamentally spleen and liver, and (ii) adult-specific EMH in non-fetal hematopoietic sites.

EMH in non-fetal hematopoietic sites can arise either spontaneously as a benign tumor possibly driven by a stromal population [2,3], or upon extreme hematopoietic demand [4]. Benign EMH masses in non-fetal hematopoietic sites occur with a particular high frequency in the adrenal gland, constituting a distinct clinical entity called adrenal myelolipoma, with a prevalence at autopsy estimated to be around 0.08 to 0.2% [3]. Myelolipomas are disproportionally associated with congenital adrenal hyperplasia (with a prevalence of up to 6% [5]) a condition that associates high circulating adrenocorticotropic hormone (ACTH) levels [6].

We hypothesized that exogenous hormonal stimulation may induce a hematopoietic niche in the adrenal glands. We show that the murine adrenal gland can be induced by ACTH to form a hematopoietic-supportive tissue and used as a model to study the components of a minimalistic adult hematopoietic niche, bypassing the need for an ossified structure. EMH-induced adrenal glands contain serially transplantable HSPCs, host HSPCs upon adrenal induction within newly formed PDGFRα+ stromal niches and retain CD45+ hematopoietic cells in a CXCR4-dependent manner. CXCL12-GFP reporter mice reveal numerous CXCL12+ stromal cells with reticular morphology within the adrenal gland resembling CXCL12-Abundant Reticular (CAR) cells.

Furthermore, we show that human myelolipoma samples also contain an abundant CXCL12+ population, mirroring the findings of our murine model.

Methods summary

Detailed experimental methods are provided in the Supplemental material file.

Surgery

For splenectomy, animals were placed on their right flank. The spleen was exposed, and the splenic vessels were ligated. Then, the spleen was removed. A minimal period of seven days was observed before starting any experiment.

EMH induction cocktail and inhibitors

For induction of EMH in the adrenal gland, mice were injected daily for 20-21 days with G-CSF (150 µg/kg filgrastim Neupogen 30mio U/0.5ml Amgen, diluted in Glucosum Bichsel solution 5 % or NaCl 0.9% as vehicle), testosterone (310 µg/mouse, testosterone undécanoate NEBIDO 1000 mg/4 ml Bayer diluted in corn oil sigma C8267-500ml for a final volume of 30 µl subcutaneously) and ACTH (tetracosactide 20 µg/mouse subcutaneously combined with testosterone or corn oil vehicle - Synacthen Depot susp injectable 1 mg/ml Alfasigma).

Colony forming unit assay (CFU)

For CFU assays from BM cells, 10.000 CD45+ were plated in methylcellulose and assessed upon 8 days of culture.

Homing assay CXCR4i

After EMH-induction in wildtype C57BL/6J recipient mice, we FACS-sorted 35.000 GFP+ LKS cells (B6.ACTB-GFP) per recipient mouse into PBS plus 2% FBS. We incubated the GFP+ LKS cells with plerixafor 1 µM (AMD3100, Selleckchem) and injected them intravenously [7]. At 30 min, 12 and 24 hours post-LKS injection we administered plerixafor dissolved in PBS (10

mg/kg) intraperitoneally to recipient mice, as previously described [8]. At 36 hours post-LKS injection, the adrenal glands were collected.

Histology

For IHC, detection was performed manually with DAB (3,3′-Diaminobenzidine, D5905, Sigma-Aldrich) or Discovery purple/Discovery teal. Sections were counterstained with Harris or Mayer hematoxylin.

Immunofluorescence and confocal microscopy

Harvested adrenal glands were cut to 200 µm-thick whole-mount sections, that were imaged with a Leica STELLARIS V.

For adrenal sections, OCT-embedded organs were cut into 5-micron thick sections and imaged with a Nikon Ti2 spinning-disk confocal microscope. All antibodies used can be found in Supplementary Methods Table 1.

Quantification and statistics

p-values were calculated using unpaired two-tailed Student's t-test or one-way ANOVA with GraphPad Prism 9. *, p-value<0.05; **, p-value<0.01; ***, p-value<0.001; ****, p-value<0.0001.

For human data All procedures were in accordance with the ethical standards of the responsible committee on human experimentation and in accordance with the 1975 Helsinki declaration as revised in 2008. The local ethical commission approved the study (CER-VD, Lausanne, Switzerland) and a specific consent for this study was obtained in cases where a general consent for research was not already available. For cases where the effort to obtain a specific consent were disproportionate, specific consent was waived by the CER-VD according to the provision of the Swiss Federal Human Research Ordinance (HRO, RS

810.301). For animal studies Experiments were carried out in accordance with the Swiss law and with approval of the cantonal authorities (Service Vétérinaire de l'Etat de Vaud) and ARRIVE guidelines.

Results

The adrenal gland can be hormonally induced to host hematopoietic cells

The description of adrenal myelolipomas as boneless EMH masses in several mammalian species prompted us to hypothesize that the adult adrenal gland could be induced into an adult-specific hematopoietic supportive environment. Selye and Stone described in 1950 the possibility of transforming the adrenal gland into myeloid-like tissue through stimulation with pituitary gland extracts, testosterone and tumor lysates[9].

Based on this model, we designed a strategy to induce EMH in the murine adrenal gland. We injected a hematopoietic cytokine (Granulocyte colony-stimulating factor (G-CSF)) and the pituitary axis adrenal-corticotropic hormone (ACTH) as well as an androgen (testosterone undecanoate) in splenectomized mice (Figure 1A). Mice developed symptoms of hypercortisolism (Cushing syndrome) within the first seven days of injection, showing increased weight, polyuria and polydipsia [10] (Supplementary Figure 1A, B). EMH induction treatment modestly increased circulatory white blood cells and granulocytes, as expected upon G-CSF administration, but had no effect on hemoglobin (Supplementary Figure 1C-E).

Adrenal glands from induced mice were markedly larger than those from the control group (Figure 1B). Upon H&E histological examination, foci of hematopoietic cells could be identified morphologically in the adrenal cortex of EMH-induced mice (Figure 1C) and further confirmed with IHC for CD45, a pan-hematopoietic marker (Figure 1D). EMH was not detected in kidney, pancreas, ovary, white adipose tissue, brown adipose tissue, or omentum. We did find, however, foci in the liver, which are congruent with the described induction of

EMH in this organ upon G-CSF treatment[11]. These foci were morphologically similar to those found in the adrenal glands, and contained small, basophilic cells with a low cytoplasm-to-nucleus ratio (Supplementary Figure 1F). We found cells positive for vWF, a marker of megakaryocytes, suggesting *in situ* hematopoiesis (Supplementary Figure 1G). As EMH foci contain small cells that could resemble lymphocytes, we performed IHC for CD3 and B220 in the adrenal glands to rule out a lymphocytic infiltrate. Both markers were predominantly negative in the EMH foci of the adrenal glands (Supplementary Figure 1H). Conversely, we found Ter119 positive cells in the EMH foci of the induced adrenal glands, indicating nucleated cells of erythroid identity (Supplementary Figure 1H). While Selye and Stone mentioned the presence of adipocytes in the induced adrenal glands of their rat model, we could not detect mature adipocytes in our samples. The increased number of hematopoietic cells in the induced adrenal glands was quantified by flow cytometry (Figure 1E), which revealed a 4-fold increase in CD45+ cells in the glands retrieved from the treated group.

Colony-forming unit (CFU) assays measure the progenitor function of short-term HSPCs [12]. This assay showed that cells within the induced adrenal glands form more colonies than those obtained from the control glands, accounting for a 15-fold increase in total colonies (Figure 1F). The increase in CFUs was statistically significant also when normalized to the total CD45+ count to take into consideration the increased adrenal volume and thus higher numbers of CD45+ cells in the induced glands (Supplementary Figure 1I). Both the induction cocktail and splenectomy were necessary for the full development of the phenotype (Figure 1G and Supplementary Figure 1J). Collectively, these

results indicate that the adrenal glands can be hormonally induced to selectively enrich in hematopoietic cells with increased colony-forming potential.

The induced adrenal gland contains functional, serially transplantable HSPCs

Once we had determined the presence of hematopoietic cells with CFU potential, we investigated the nature of the hematopoietic cells found in the induced adrenal glands. For this we performed flow cytometry for known HSPC surface markers. Within the BM, the immunophenotype of the progenitor cells, defined as lineage- c-Kit+ Sca-1+ (LKS), showed no difference between control and induced mice (Figure 2A). In blood, the induction cocktail caused an increase in circulating c-Kit+ progenitor cells, as expected due to G-CSF administration. In the adrenal gland, a different surface marker profile was observed. CD45+ lineage- cells obtained from the induced adrenal glands did not show the same surface marker profile as in the BM, but instead a proportion of them displayed a c-Kit^{low} and Sca-1^{+} profile (Figure 2A). This is congruent with previous reports that have shown a decrease in the expression of c-Kit in splenic HSCs [13]. We then interrogated the cells in this gate for the presence of the SLAM markers CD150 and CD48[14], which are used to identify multipotent progenitors (MPPs; LKS CD150^{-}CD48$^{+/-}$) and hematopoietic stem cells (HSCs; LKS CD150^{+}CD48^{-}) in the murine BM. In doing so, we observed both LK^{lo}S CD150+CD48- cells and LK^{lo}S (CD150^{-}CD48$^{+/-}$) (Supplementary Figure 2A). This immunophenotypical signature suggests that HSPCs are present in the EMH-induced adrenal gland. However, due to the limited number of hematopoietic cells in the adrenal glands and the seemingly lower expression of their markers, cell sorting could not be performed to investigate the functional

capacities of the lineage- populations present in the induced adrenal glands. Instead, we performed functional transplantation assays.

CD45.2 donor mice were thus treated with the EMH induction cocktail, and the cells obtained by enzymatic digestion of the adrenal glands were directly transplanted together with CD45.1/.2 BM competitor cells into lethally irradiated CD45.1 recipient mice. Based on the CFU data (Figure 1F), 6 adrenal glands contain a similar colony-forming potential as 125.000 total BM, the minimal BM cell rescue dose in our experimental setup. Therefore, we transplanted the total cellular content of 6 adrenal glands -control or EMH-induced- together with 125.000 total BM competitor cells for a 1:1 competitive transplant assay. CD45.2+ cells in the blood of the CD45.1 primary recipient indicate engraftment originating from our donor mice and thus reveal adrenal resident HSPCs (Figure 2B). We observed a significant CD45.2 engraftment exclusively for mice receiving CD45.2 donor cells from EMH-induced adrenal glands, but not from control adrenal glands (Figure 2C). Donor cells gave rise to both myeloid and lymphoid circulating blood cells (Supplementary Figure 2B). More importantly, CD45.2 cells obtained from EMH-induced adrenal glands were serially transplantable and capable of producing circulating cells up to at least tertiary transplants (Figure 2C). Long-term CD45.2 engraftment was also observable in the BM of mice receiving cells from EMH-induced donors, thereby serving as proof for the presence of functional HSPCs in the EMH-induced adrenal glands but not the uninduced controls (Figure 2D).

Induced adrenal glands recruit circulating HSPCs

After identifying the hematopoietic supporting capacity of the induced adrenal glands, we sought to define the source of the observed HSPCs.

Embryologically, the aorta-gonad-mesonephros (AGM) structure gives rise to both the definitive HSPCs and the adrenal cortex. During embryonic development, in the AGM, HSPCs derive from endothelial cells in an endothelial-to-hematopoietic (EHT) transition [15]. Even if unlikely, we wanted to exclude that the HSPCs we observed in the adrenal glands could develop *in situ* from non-hematopoietic adrenal cells upon EMH induction. To test this hypothesis, we transplanted splenectomized mice with GFP+ total BM cells to obtain a mouse with a GFP+ hematopoietic system. After recovery post transplantation, mice were treated with the EMH induction cocktail for 20 days (Figure 3A). If direct metaplasia occurred, adrenal HSPCs would be GFP- upon EMH-induction, while BM HSPCs would be GFP+. As in previous assays, CFU assays showed the presence of hematopoietic progenitors in the induced adrenal glands (Figure 3B), but not in control mice, as well as in the BM of all mice (Figure 3C). It should be noted that the baseline number of colonies was reduced by about 50% in irradiated mice as compared to all other experiments performed in non-irradiated EMH-induced adrenal glands. Close to 100% of all colonies present in the adrenal gland CFU assays were GFP+, indicating a BM origin of the hematopoietic cells in the adrenal gland upon EMH induction. Overall, these results indicate that HSPCs found in the adrenal gland are recruited from the BM into the induced adrenal gland and do not arise *de novo* in the organ.

CXCL12 is required for homing and retention of hematopoietic cells in the induced adrenal gland

Once we had determined that the induced adrenal gland can be colonized by hematopoietic cells with CFU potential originating from the BM, we

hypothesized that the CXCL12-CXCR4 axis would be involved in this phenomenon, given its crucial role in homing of hematopoietic progenitor cells to the BM [8]. To evaluate this hypothesis, we used plerixafor, a pharmacological antagonist of CXCR4. We performed the EMH-induction protocol and then injected the EMH-induced mice with 35.000 GFP+ LKS cells treated with plerixafor. We administered plerixafor intraperitoneally at 30 min, 12 hours and 24 hours post-LKS injection [8]. The mice were sacrificed 36 hours post-LKS injection and the adrenal glands evaluated for CD45+ counts and GFP+ CFU potential (Figure 3D). We expected plerixafor to hamper the colonization of the adrenal niche by the injected GFP+ LKS cells, and therefore a decrease in the number of GFP+ cells produced in the CFU assay. Congruently, upon EMH-induction, we observed a marked decrease in the number of CD45+ cells in the adrenal glands of induced mice treated with plerixafor (Figure 3E), indicating that the CXCL12-CXCR4 axis is necessary for the retention of CD45+ cells in the adrenal niche. We then evaluated by flow cytometry the proportion of GFP+ cells within the colonies. Consistent with our hypothesis, we observed a decrease in the percentage of GFP+ cells that composed the hematopoietic colonies in EMH-induced animals treated with plerixafor (Figure 3F), indicating that the CXCL12-CXCR4 axis is required not just for the retention but also for the homing of hematopoietic cells with CFU potential to the adrenal gland.

Finally, we looked into the presence of CXCL12-abundant reticular (CAR) cells in the adrenal gland, which have been described to be essential for hematopoietic support and retention in the BM [16]. For this, we took advantage of the extensively characterized CXCL12-GFP knock-in murine reporter model [17]. We identified GFP+ cells in both the induced and non-induced adrenal gland by

flow cytometry (data not shown) and confirmed our findings with whole mount confocal microscopy (Figure 4A control, 4B EMH-induced). These cells were of reticular morphology, reminiscent of CAR cell morphology in the BM [18]. Surprisingly, and despite the effect of CXCR4 blockage in induced as compared to non-induced adrenal glands, we observed no obvious differences in CXCL12-GFP+ (CAR) cell numbers or morphology between groups. Taken together, our results show that the adrenal stroma shares immunophenotypic features with the BM stroma and contains CAR-like CXCL12+ cells. Furthermore, our data is compatible with hematopoietic cells being actively retained in the adrenal niche by CXCL12-CXCR4 signaling.

The adrenal stroma is modified by the EMH-induction cocktail

Our data granted further examination of the stroma of the adrenal gland. For this, we examined a recently published publicly available single-nuclei transcriptomics dataset of the murine adrenal gland, including two adrenal stroma clusters [19]. We found that the adrenal stroma expresses *Pdgfra* (which encodes for the protein PDGFRα) as well as hematopoietic-supportive genes such as *Cxcl12* (Figure 5A).

The transcriptomics data prompted us to functionally interrogate the intrinsic hematopoietic-supportive capacity of the uninduced adrenal stroma. For this, we conducted *in vitro* coculture studies with FACS-sorted HSPCs (LKS cells) from the BM plated on adrenal plastic-adherent cells and measured the CD45+ cell output after 7 days of coculture in the absence of additional cytokines. LKS cells plated on adrenal plastic-adherent cells produced a larger CD45+ progeny than those plated on monolayers of BM stromal cells (BMSCs)

or cultured alone (Figure 5B). Our results suggest that plastic-adherent cells from the adrenal stroma may be intrinsically supportive of hematopoiesis.

Then, we examined *in situ* EMH-induced adrenal glands for stromal markers known to be associated with the hematopoietic BM niche, including PDGFRα, in line with previous reports of mesoderm-derived stromal cells regulating the emergence of the AGM hematopoietic niche [20]. Indeed, staining for PDGFRα showed a marked reorganization of the adrenal cortical stroma in the EMH-induced organs surrounding foci of small, tightly packed nuclei that were morphologically reminiscent of EMH in H&E-stained sections (Supplementary Figure 3A). The cell clusters within the PDGFRα stromal nodules were positive for CD45+, confirming the identity of the hematopoietic foci (Figure 5C). Moreover, and surprisingly, we observed a certain degree of colocalization of PDGFRα with Leptin receptor (LepR) exclusively in the stromal clusters for EMH-induced adrenal glands, with PDGFRα+LepR+ stromal cells located in pericyte position as defined by endomucin+ endothelial cells (Figure 5D and Figure 5D inset; single-channel images and the DAPI overlay are provided in Supplementary Figure 3B). As LepR is a commonly used marker to identify the BM stroma[21], our results hint at the possibility of inducing a BM stroma-like phenotype in the adrenal stroma. Finally, we interrogated the EMH-induced adrenal glands for cells positive for markers of HSPCs in the PDGFRα nodules. For this, we stained sections with c-Kit and PDGFRα and observed that the nodules did contain rare c-Kit+ cells, corroborating our transplantation data (Figure 5E).

Together, our data show that the EMH induction cocktail triggers marked changes in the adrenal stroma architecture, with formation of PDGFRα+LepR+/-

clusters encompassing hematopoietic foci capable of hosting rare c-Kit+ HSPCs, and thus potentially enhancing the intrinsic hematopoietic-supportive capacity of the adrenal stroma *in vivo*.

Human myelolipoma is positive for BM stroma markers and contains CXCL12+ reticular cells

Myelolipoma, a benign tumor composed of adipose and hematopoietic tissues, is frequently found in the adrenal gland, particularly in the context of endocrine disorders that associate elevated ACTH levels. We hypothesized that human myelolipomas might recapitulate a phenomenon like the one we observe in the adrenal gland of mice treated with our EMH-induction cocktail. For this, we retrieved myelolipoma samples originally collected at the Centre Hospitalier Universitaire Vaudois (CHUV), Lausanne, Switzerland. The clinical characteristics of our myelolipoma cohort are summarized in Supplementary Table 1, including the anatomical origin of the myelolipomas, of which 60% were adrenal and 40% pelvic or retroperitoneal. We then compared our samples with the published registry gathering all reported data cases of adrenal myelolipoma, recently published by Decmann et al [22] (Table 1). Surprisingly, we found that 20% of the patients in our cohort had a history of splenectomy (n=2 out of 10) whereas the previously published prevalence of splenectomy in the general population is around 0.4% [23].

We performed immunohistochemistry (IHC) studies of our myelolipoma samples using a panel of markers designed to evaluate known components of the human BM stroma, namely CD73, CD90, CD146, CD271, CXCL12 and Nestin, as well as CD34 to target hematopoietic progenitors [24–26].

Using paraffin-embedded samples stored from the diagnostic workup of our patients, we stained consecutive sections and examined the presence of positive cells in IHC. We included, as controls, human BM and an adrenal adenoma. CD34 and CD90 were expressed in only a fraction of our samples. CD73, CD146 and CD271 and Nestin were expressed across all samples (Supplementary Figure 4 and Supplementary Figure 5A). Notably, CXCL12 was present in all myelolipoma samples (Figure 6A and Table 1) but not in the adrenal adenoma control. Furthermore, CXCL12+ cells were of reticular morphology and co-expressed the transcription factor FOXC1, the best characterized master regulator of hematopoietic support factor expression in BM niche cells [27] to a similar extent as the BM stroma, which was not the case for healthy adrenal glands or adrenal adenomas (Figure 6B). This stain was specific, as illustrated in Supplementary Figure 5B-C. Taken together, our results indicate the reproducible detection of CXCL12+ stromal cells in human myelolipoma samples with similar characteristics to BM stroma. Thus, our data supports the use of adrenal myelolipomas as a surrogate to understand the composition of an inducible supportive hematopoietic niche, which mirrors our inducible adrenal niche model.

Discussion

Here we show that the adrenal gland can be transformed into a hematopoietic supportive environment and used as a model to study the minimal stromal components of a non-ossified *de novo* hematopoietic niche. The EMH-induced adrenal niche contained CXCL12+ cells with classical reticular morphology, concomitant to the formation of PDGFRα+LepR+/- stromal clusters which associated to tightly packed, cobblestone-like hematopoietic

colonies containing rare c-Kit+ HSPCs, including serially transplantable stem cells. Our findings are supported by the presence of CAR-like CXCL12+FOXC1+ reticular cells in human adrenal myelolipoma, associated to CD34+ HSPCs.

The observation that the adult adrenal gland can support hematopoiesis upon hormonal stimulation is particularly interesting as the adrenal cortex originates from the AGM, the structure that gives rise to definitive HSCs during embryonic development, with critical involvement of environmental cues provided by mesoderm-derived PDGFRα+ stromal cells [20]. The adrenal gland is therefore ontogenically related to a hematopoietic supportive structure and can be transformed into an adult niche, a phenomenon that has been clearly described in the spleen and the liver [2]. Moreso, it has been recently shown in a human cell atlas of fetal gene expression, that the fetal adrenal gland contains limited erythropoiesis, pointing to a previously overlooked hematopoietic supportive capacity of the adrenal gland [28]. Furthermore, the propensity of myelolipoma to develop in the adrenal gland suggests a specific hematopoietic supportive population in this location. Adrenal myelolipoma has been proposed to originate from a mesenchymal progenitor cell giving rise to the stromal compartment and then recruiting hematopoietic cells[29], something that would be in line with our observations.

We initially attempted to fully recapitulate myelolipomas in mice with both the adipocytic compartment and hematopoietic cells. Based on historical publications using rats as models and crude pituitary extracts as stimulants, we developed a model using chemically defined hormonal stimulation in splenectomized mice. G-CSF was used to simulate stress hematopoiesis. G-

CSF treatment alone directly stimulates HSPCs proliferation and mobilization, accelerating exit of severe neutropenia by an average of 3-6 days in humans [30,31]. In accordance with the Selye and Stone's [9] original description, our cocktail also contained testosterone. The effect of androgens as a stimulant of hematopoiesis has been thoroughly described and is used in patients to treat BM insufficiency, specifically in the context of telomeropathies and Fanconi anemia [32–35]. Instead of pituitary extracts, ACTH daily was chosen to induce EMH in the adrenal gland because the incidence of myelolipoma increases several-fold in patients suffering from congenital adrenal hyperplasia, a disease of the cortisol axis that increases the levels of ACTH [22]. Consequently, our induction cocktail is based on stimulation of both the adrenal gland, with ACTH, and the hematopoietic system, with G-CSF and testosterone. We however failed to observe adipocytes in our model, which suggests that mature adipocytes might not be necessary for hematopoietic support in the adrenal EMH. Finally, we found that splenectomy was necessary for the full induction of EMH in the adrenal gland. As the spleen is a known site of physiological EMH in mice[36], we speculate that its presence might retain circulating HSPCs that would otherwise colonize the adrenal gland in our model.

In our collection of human adrenal myelolipoma samples, patients presented similar characteristics as published in the literature. Interestingly, we found an overrepresentation of splenectomized patients in our myelolipoma cases. While the cohort is small, and this could be an incidental finding, it could play a role in the development of myelolipoma. An in-house IHC-based panel, based on markers described for the BM stroma, consistently showed the presence of CXCL12-expressing cells with reticular morphology which co-

expressed FOXC1 in the myelolipomas. Both proteins have been reported as markers of BM stromal cell populations capable of providing hematopoietic support, with CXCL12 having a known mechanistic role in this function, and FOXC1 acting as a master regulator of hematopoietic-supporting stromal niche cells [27].

In conclusion, we present our model as a novel tool to increase our understanding of the physiology of hematopoietic support and to facilitate the study of inducible, adult-specific niche models. From a phylogenetic standpoint, examples of adult-specific hematopoietic niches outside of the BM exist in vertebrate evolution, and appear as early as in jawless fish in the form of the dorsal fat body [37]. The composition of what constitutes the simplest unit of hematopoietic niche, supporting both HSC self-renewal and progenitor expansion, remains largely unknown. Since the exact composition needed to recapitulate *enough* complexity of the hematopoietic microenvironment for it to be functional is still undefined, further understanding of minimalistic niches, like the inducible boneless adrenal niche one we report, has the potential to aid in the development of biomedical and tissue engineering applications.

Acknowledgement

FS was funded by the SNSF MD-PhD grant 183986. ON was funded by SNSF Professorship grants PP00P3_144857, PP00P3_176990 and PP00P3_183725 and, together with AAC, by the University of Lausanne (UNIL). We wish to thank Josefine Tratwal, Paolo Bianco, Mukul Girotra, Shanti Rojas-Sutterlin, Marian Manongdo and Markus Manz for help in the inception of the project, and for providing critical advice along its development. This project would not have been possible without the support of the EPFL animal facility

(CPG) and the animal caretakers, in particular Laetitia Cagna, Margaux Mouchet and Pierre Dodane. We thank the EPFL and UNIL flow cytometry facilities, in particular Danny Labes, the members of the EPFL histology facility and the EPFL Biomolecular Screening Facility. We thank Dr. Nathalie Piazzon (Institut de Pathologie Biobank, UNIL/CHUV, Lausanne) for facilitating the access to human myelolipoma samples. We thank Dr. Takashi Nagasawa, Graduate School of Frontier Biosciences and Graduate School of Medicine, Osaka University, Japan, for the generous gift of the CXCL12/GFP knock-in mice

This research was funded in whole or in part by the Swiss National Science Foundation (SNSF) [Grant numbers: 183986, PP00P3_144857, PP00P3_176990 and PP00P3_183725]. For the purpose of Open Access, a CC BY public copyright licence is applied to any Author Accepted Manuscript (AAM) version arising from this submission.

Authors contribution

ON and FS conceived the ideas and obtained funding for the project. FS performed all the experiments with the help of AAC, SFL and AO. FS, ON and AAC analyzed the results and wrote the manuscript. AV and CNA performed and analyzed all wholemount confocal microscopy imaging presented in this manuscript. RS, CB, JSD and LdL set up the immunostaining panel for human myelolipomas. SG assessed the myelolipoma images. FS and ON compiled the clinical data. First co-authorship was granted based on the final contribution to the completion of the project; FS developed the experimental pipelines and executed the experiments while AAC assisted during the experiments and was

involved in the preparation of the manuscript, analysis of the data and finalization of the project.

Conflict of interest statement:

The authors declare no conflict of interest for this project

References

1. Yamamoto K, Miwa Y, Abe-Suzuki S, et al. Extramedullary hematopoiesis: Elucidating the function of the hematopoietic stem cell niche (Review). *Molecular Medicine Reports*. 2016;13(1):587–591.
2. Johns JL, Christopher MM. Extramedullary hematopoiesis: a new look at the underlying stem cell niche, theories of development, and occurrence in animals. *Vet Pathol*. 2012;49(3):508–523.
3. Palmer WE, Gerard-McFarland EL, Chew FS. Adrenal myelolipoma. *AJR Am J Roentgenol*. 1991;156(4):724.
4. Hisamud-din N, Mustafah NM, Fauzi AA, Hashim NM. Incomplete paraplegia caused by extramedullary hematopoiesis in a patient with thalassemia intermedia. *Spinal Cord Ser Cases*. 2017;3(1):17020.
5. Nermoen I, Rørvik J, Holmedal SH, et al. High frequency of adrenal myelolipomas and testicular adrenal rest tumours in adult Norwegian patients with classical congenital adrenal hyperplasia because of 21-hydroxylase deficiency. *Clin. Endocrinol. (Oxf)*. 2011;75(6):753–759.
6. Claahsen - Van Der Grinten HL, Speiser PW, Ahmed SF, et al. Congenital Adrenal Hyperplasia—Current Insights in Pathophysiology, Diagnostics, and Management. *Endocrine Reviews*. 2022;43(1):91–159.
7. Christopherson KW, Hangoc G, Mantel CR, Broxmeyer HE. Modulation of Hematopoietic Stem Cell Homing and Engraftment by CD26. *Science*. 2004;305(5686):1000–1003.
8. Nombela-Arrieta C, Pivarnik G, Winkel B, et al. Quantitative imaging of haematopoietic stem and progenitor cell localization and hypoxic status in the bone marrow microenvironment. *Nat Cell Biol*. 2013;15(5):533–543.
9. Selye H, Stone H. Hormonally Induced Transformation Of Adernal into Myeloid Tissue. *Am J Pathol*. 1950;26(2):211–233.
10. Pivonello R, De Martino MC, De Leo M, Simeoli C, Colao A. Cushing's disease: the burden of illness. *Endocrine*. 2017;56(1):10–18.
11. Mendt M, Cardier JE. Role of SDF-1 (CXCL12) in regulating hematopoietic stem and progenitor cells traffic into the liver during extramedullary hematopoiesis induced by G-CSF, AMD3100 and PHZ. *Cytokine*. 2015;76(2):214–221.
12. Purton LE, Scadden DT. Limiting factors in murine hematopoietic stem cell assays. *Cell Stem Cell*. 2007;1(3):263–270.
13. Coppin E, Florentin J, Vasamsetti SB, et al. Splenic hematopoietic stem cells display a pre-activated phenotype. *Immunol Cell Biol*. 2018;96(7):772–784.
14. Oguro H, Ding L, Morrison SJ. SLAM Family Markers Resolve Functionally Distinct Subpopulations of Hematopoietic Stem Cells and Multipotent Progenitors. *Cell Stem Cell*. 2013;13(1):102–116.
15. Ottersbach K. Endothelial-to-haematopoietic transition: an update on the process of making blood. *Biochem Soc Trans*. 2019;47(2):591–601.
16. Greenbaum A, Hsu Y-MS, Day RB, et al. CXCL12 in early mesenchymal progenitors is required for haematopoietic stem-cell maintenance. *Nature*. 2013;495(7440):227–230.
17. Ara T, Tokoyoda K, Sugiyama T, et al. Long-Term Hematopoietic Stem Cells Require Stromal Cell-Derived Factor-1 for Colonizing Bone Marrow during Ontogeny. *Immunity*. 2003;19(2):257–267.

18. Gomariz A, Helbling PM, Isringhausen S, et al. Quantitative spatial analysis of haematopoiesis-regulating stromal cells in the bone marrow microenvironment by 3D microscopy. *Nat Commun*. 2018;9(1):2532.
19. Bedoya-Reina OC, Li W, Arceo M, et al. Single-nuclei transcriptomes from human adrenal gland reveal distinct cellular identities of low and high-risk neuroblastoma tumors. *Nat Commun*. 2021;12(1):5309.
20. Chandrakanthan V, Rorimpandey P, Zanini F, et al. Mesoderm-derived PDGFRA+ cells regulate the emergence of hematopoietic stem cells in the dorsal aorta. *Nat Cell Biol*. 2022;24(8):1211–1225.
21. Zhou BO, Yue R, Murphy MM, Peyer JG, Morrison SJ. Leptin-Receptor-Expressing Mesenchymal Stromal Cells Represent the Main Source of Bone Formed by Adult Bone Marrow. *Cell Stem Cell*. 2014;15(2):154–168.
22. Decmann Á, Perge P, Tóth M, Igaz P. Adrenal myelolipoma: a comprehensive review. *Endocrine*. 2018;59(1):7–15.
23. Jais X, Ioos V, Jardim C, et al. Splenectomy and chronic thromboembolic pulmonary hypertension. *Thorax*. 2005;60(12):1031–1034.
24. Tormin A, Li O, Brune JC, et al. CD146 expression on primary nonhematopoietic bone marrow stem cells is correlated with in situ localization. *Blood*. 2011;117(19):5067–5077.
25. Sacchetti B, Funari A, Michienzi S, et al. Self-Renewing Osteoprogenitors in Bone Marrow Sinusoids Can Organize a Hematopoietic Microenvironment. *Cell*. 2007;131(2):324–336.
26. Méndez-Ferrer S, Battista M, Frenette PS. Cooperation of β2- and β3-adrenergic receptors in hematopoietic progenitor cell mobilization: β-adrenoceptors in bone marrow microenvironment. *Annals of the New York Academy of Sciences*. 2010;1192(1):139–144.
27. Omatsu Y, Seike M, Sugiyama T, Kume T, Nagasawa T. Foxc1 is a critical regulator of haematopoietic stem/progenitor cell niche formation. *Nature*. 2014;508(7497):536–540.
28. Cao J, O'Day DR, Pliner HA, et al. A human cell atlas of fetal gene expression. *Science*. 2020;370(6518):.
29. Feng C, Jiang H, Ding Q, Wen H. Adrenal myelolipoma: A mingle of progenitor cells? *Medical Hypotheses*. 2013;80(6):819–822.
30. Harousseau JL, Witz B, Lioure B, et al. Granulocyte colony-stimulating factor after intensive consolidation chemotherapy in acute myeloid leukemia: results of a randomized trial of the Groupe Ouest-Est Leucémies Aigues Myeloblastiques. *J. Clin. Oncol.* 2000;18(4):780–787.
31. Godwin JE, Kopecky KJ, Head DR, et al. A double-blind placebo-controlled trial of granulocyte colony-stimulating factor in elderly patients with previously untreated acute myeloid leukemia: a Southwest oncology group study (9031). *Blood*. 1998;91(10):3607–3615.
32. Bär C, Huber N, Beier F, Blasco MA. Therapeutic effect of androgen therapy in a mouse model of aplastic anemia produced by short telomeres. *Haematologica*. 2015;100(10):1267–1274.
33. Townsley DM, Dumitriu B, Liu D, et al. Danazol Treatment for Telomere Diseases. *N Engl J Med*. 2016;374(20):1922–1931.
34. Català A, Ali SS, Cuvelier GDE, et al. Androgen therapy in inherited bone marrow failure syndromes: analysis from the Canadian Inherited Marrow Failure Registry. *Br J Haematol*. 2020;189(5):976–981.

35. Kirschner M, Vieri M, Kricheldorf K, et al. Androgen derivatives improve blood counts and elongate telomere length in adult cryptic dyskeratosis congenita. *Br. J. Haematol.* 2021;193(3):669–673.
36. Schubert TEO, Obermaier F, Ugocsap P, et al. Murine Models of Anaemia of Inflammation: Extramedullary Haematopoiesis Represents a Species Specific Difference to Human Anaemia of Inflammation That Can Be Eliminated by Splenectomy. *Int J Immunopathol Pharmacol*. 2008;21(3):577–584.
37. Craft CS, Scheller EL. Evolution of the Marrow Adipose Tissue Microenvironment. *Calcif Tissue Int*. 2017;100(5):461–475.

Tables

Sample ID	CD34	CD73	CD90	CD146	CD271	CXCL12	NESTIN	Anatomical origin
A	+	/	+++	+++	/	++	+++	Adrenal
B	-	+	-	++	+	+	++	Retroperitoneum
C	+	+	+	+++	+++	++	++	Pelvic
D	-	+	+	++	+++	+++	+	Adrenal
E	-	+++	+++	+++	+++	+	+++	Adrenal
F	-	++	++	+++	+++	+	+++	Adrenal
G	-	++	+	++	+++	-	+++	Adrenal (adenoma)
H	-	++	+	++	+++	+	+++	Adrenal
I	+	+++	+	++	+++	+	++	Pelvic
J	-	+	+	+	++	-	+	Bone marrow
K	+	+	++	++	+++	+	+++	Adrenal

Table 1.

Detailed semiquantitative histological characteristics of the different immunohistochemical stains on the myelolipoma samples and two controls (healthy BM (J) and adrenal adenoma (G)), quantification represent number of positive cells per samples (- corresponds to no positive cell, + to +++ correspond to linearly increasing number of positive cells)

Figure legends

Figure 1. The adrenal gland can be hormonally induced to host hematopoietic cells

A General experimental design to induce EMH in the adrenal gland. **B** Macroscopic picture of freshly isolated adrenal glands. **C** Representative images of H&E stains for vehicle (top) and EMH-induced (bottom) adrenal glands. The boxed area is magnified on the right of each image. Scale bar for inset represents 30 µm. **D** Representative images of CD45 IHC stain in an adrenal gland. The boxed area is magnified on the right of each image. Scale bar for inset represents 30 µm. **E** Number of CD45+ cells per adrenal gland, measured by flow cytometry (control n=4, EMH n=6 mice, two independent experiments). **F** CFU assay, number of colonies per adrenal gland (control n=4, EMH n=6 mice, two independent experiments). **G** Number of hematopoietic colonies per adrenal gland obtained in a CFU assay from mice treated with the different components of the induction protocol (n=4 for all groups). Data are represented as mean ±SD. Differences were assessed using unpaired, two-tailed Student's *t*-test (E, F) or with one-way ANOVA followed by Holms-Sidak multiple correction test (G). P values are indicated in the graphs.

Figure 2. The adrenal gland supports functional, serially transplantable HSPCs

A Flow cytometry analysis of the BM, blood and adrenal glands of control versus EMH-treated mice, representative panels gated within the CD45+lineage negative gate are shown (control n=10, EMH n=10 mice, three independent experiments). **B** Experimental design of the competitive transplant. The total content of CD45.2+ cells retrieved from 6 adrenal glands were transplanted into a lethally irradiated CD45.1 recipient together with 125.000 CD45.1.2 total BM cells from a competitor mouse. **C, D** Evolution of the CD45.2 donor engraftment measured in peripheral blood and BM, respectively, by flow cytometry (control n=7, EMH n=8 mice, two independent experiments), Data are shown as mean ± SEM. Differences were assessed using a two-tailed unpaired Student's *t*-test.

Figure 3. The adrenal stroma recruits and supports circulating hematopoietic progenitors

A Experimental design for EMH induction after transplant with GFP+ BM. **B, C** CFU assay, number of total colonies and GFP+ colonies per single adrenal gland (**B**) and 10,000 CD45+ total BM cells (**C**) (n=6 per experimental group, two independent experiments). **D** General experimental design for homing assay. **E** CD45+ cells in EMH-induced adrenals glands retrieved from mice treated with plerixafor (CXCR4i), evaluated by flow cytometry at 16 hours post-treatment (two independent experiments, n=8 for control groups and n=10 for EMH-induced groups). **F** Percentage of GFP+ cells from the recovered cells grown in methylcellulose CFU culture after completion of the CFU assay (8 days post-plating), quantified by flow cytometry (n=9 control mice and n=8 experimental mice). Data are represented as mean ±SD and groups were compared with one-way ANOVA followed by Tukey's multiple correction test (**E**) or two-tailed, unpaired Student's *t*-test (**F**).

Figure 4. The murine adrenal gland contains CXCL12-positive cells with reticular morphology

3D Microscopy of murine adrenal glands: Representative 3D sections and optical slices of immunostained adrenal glands from (A) control-treated (n=3) and (B) EMH-induced (n=3) Cxcl12^{GFP} transgenic mice showing Endomucin (EMCN;Cyan), CXCL12-GFP (yellow) and 4′,6-diamidino-2-phenylindole (DAPI;blue). Scalebars (A) 200µm, (B) 500µm; for all cropped sections and optical slices scalebars represent 40µm.

Figure 5. EMH-induced adrenal glands have a modified stromal architecture with PDGFRa clusters hosting hematopoietic foci with rare c-kit+ HSPCs.

A, Selection of genes enriched in the PDGFRa-expressing cells of the murine adrenal gland (PDGFRa-expressing clusters: mC6 "mesenchymal" in red and mC13 "capsule" in purple, as defined by Bedoya-Reina et al. 2021). **B**, Adrenal plastic-adherent cells are supportive of CD45+ cell expansion. Expansion of total hematpoietic cells (CD45+) upon coculture for 7 days of FACS-sorted murine HSPCs (LKS) with a confluent feeder layer of BMSCs obtained from flushed, collagenase-digested bones or adrenal gland, in the absence of additional cytokines. Data are represented as mean ±SD and groups were compared with one-way ANOVA followed by Holms-Sidak multiple correction test (n=5 for LKS monoculture, 6 for BMSCs and 11 for adrenal plastic-adherent cells. Data were obtained in 2 independent

experiments). **C**, Representative images of control and EMH-induced adrenal glands (n=2-3 mice per group) stained for CD45 (green), PDGFRa (orange) and DAPI (white). Scale bars represent 20 µm in all instances in C. D**,** Representative images of control and EMH-induced adrenal glands (n=2, multiple nodules per adrenal) stained for LepR (blue), PDGFRa (orange), endomucin (teal). Yellow arrowheads indicate examples of colocalization of PDGFRa and LepR (co-localization in pink), where the latter has an elongated pattern marking cells in pericyte position, while white arrowheads indicate adrenal parenchyma cells that display a different pattern of LepR, mostly perinuclear. Scale bars represent 20 µm in all instances in **D** except for the inset, in which it represents 5 µm. **E,** Representative images of control and EMH-induced adrenal glands (n=3, multiple nodules per adrenal) stained for PDGFRa (orange), cKit (blue), and DAPI (white). Scale bars represent 20 µm in the controls, 10 µm in the EMH-induced mice. The scale bar in the inset represents 5 µm.

Figure 6. CXCL12+ cells of stromal morphology are present in human myelolipoma and co-express FOXCC1.

A. Representative images of CXCL12 IHC stains of human myelolipoma samples corresponding, from left to right, to patients I, C and D (see Table 1 for details). Scale bars correspond to 200 µm and 100 µm in the left and right columns, respectively. **B**. Double chromogenic immunohistochemical stain for CXCL12 (pink) and FOXC1 (teal) in human myelolipoma, BM, healthy adrenal gland, and adrenal adenoma. Scale bar represents 30 µm in all instances.

Figure 1

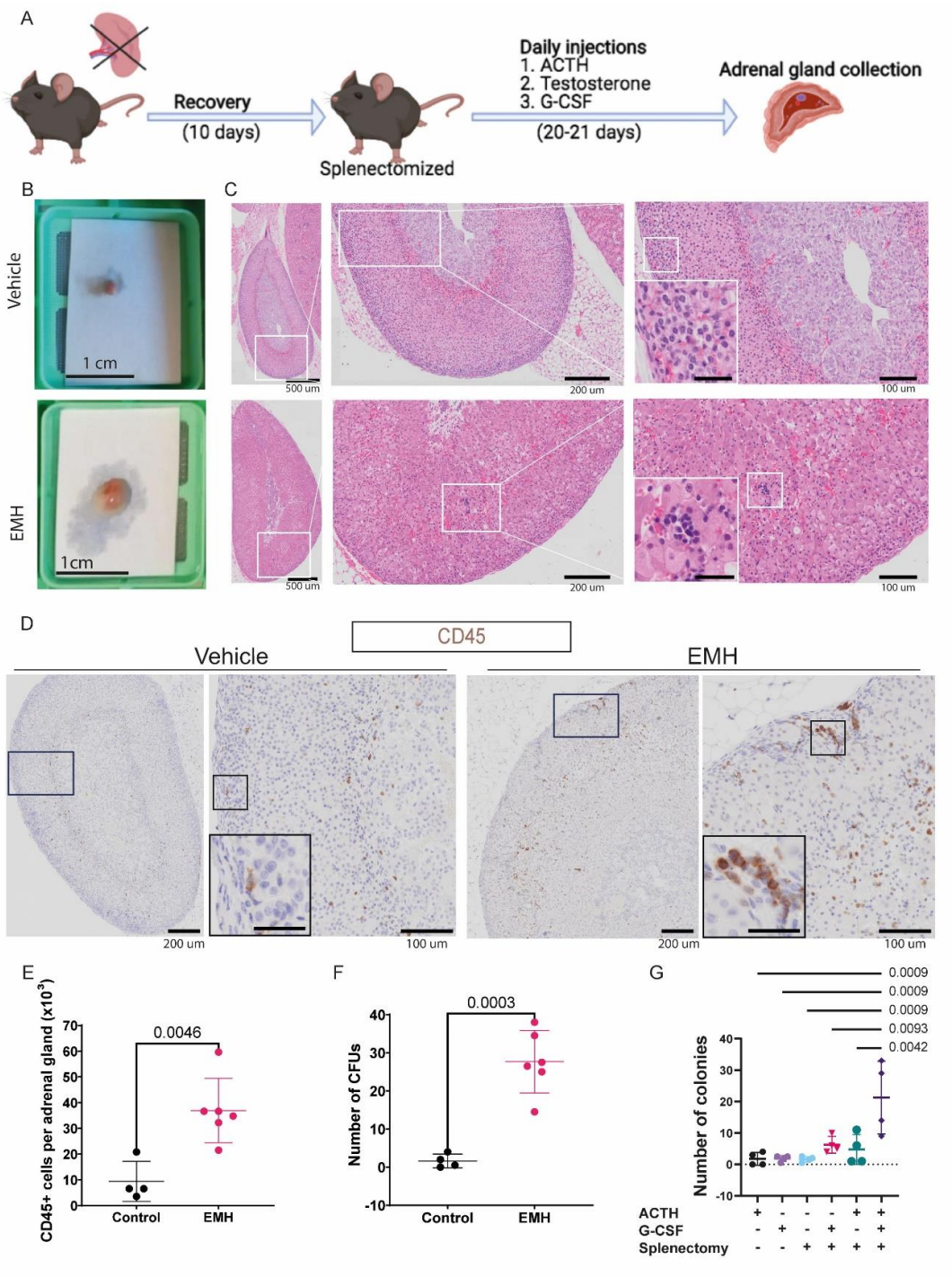

Figure 1. The adrenal gland can be hormonally induced to host hematopoietic cells

A General experimental design to induce EMH in the adrenal gland. **B** Macroscopic picture of freshly isolated adrenal glands. **C** Representative images of H&E stains for vehicle (top) and EMH-induced (bottom) adrenal glands. The boxed area is magnified on the right of each image. Scale bar for inset represents 30 µm. **D** Representative images of CD45 IHC stain in an adrenal gland. The boxed area is magnified on the right of each image. Scale bar for inset represents 30 µm. **E** Number of CD45+ cells per adrenal gland, measured by flow cytometry (control n=4, EMH n=6 mice, two independent experiments). **F** CFU assay, number of colonies per adrenal gland (control n=4, EMH n=6 mice, two independent experiments). **G** Number of hematopoietic colonies per adrenal gland obtained in a CFU assay from mice

Figure 1

treated with the different components of the induction protocol (n=4 for all groups). Data are represented as mean ±SD. Differences were assessed using unpaired, two-tailed Student's *t*-test (E, F) or with one-way ANOVA followed by Holms-Sidak multiple correction test (G). P values are indicated in the graphs.

Figure 2

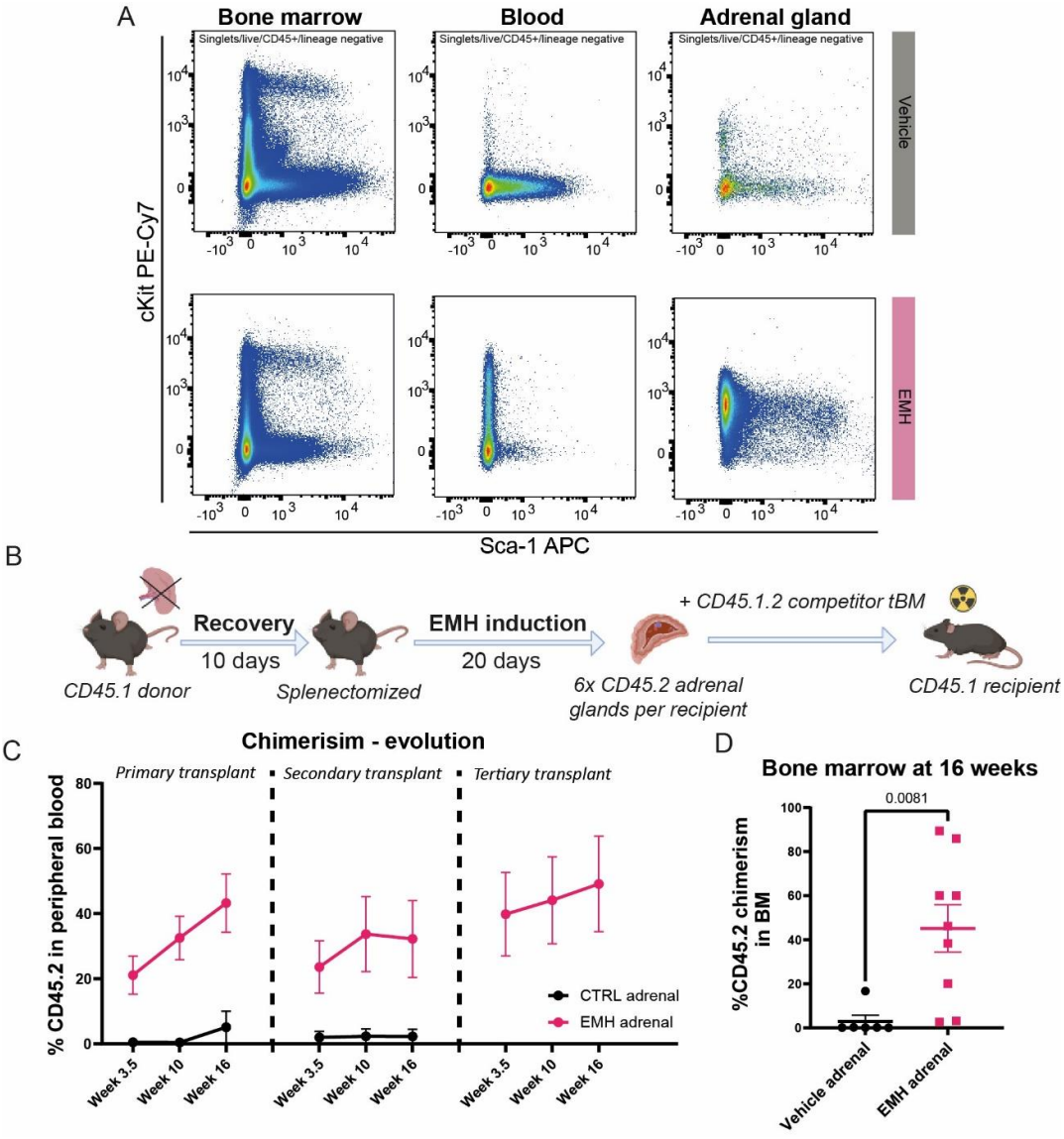

Figure 2. The adrenal gland supports functional, serially transplantable HSPCs

A Flow cytometry analysis of the BM, blood and adrenal glands of control versus EMH-treated mice, representative panels gated within the CD45+lineage negative gate are shown (control n=10, EMH n=10 mice, three independent experiments). **B** Experimental design of the competitive transplant. The total content of CD45.2+ cells retrieved from 6 adrenal glands were transplanted into a lethally irradiated CD45.1 recipient together with 125.000 CD45.1.2 total BM cells from a competitor mouse. **C, D** Evolution of the CD45.2 donor engraftment measured in peripheral blood and BM, respectively, by flow cytometry (control n=7, EMH n=8 mice, two independent experiments), Data are shown as mean ± SEM. Differences were assessed using a two-tailed unpaired Student's *t*-test.

Figure 3

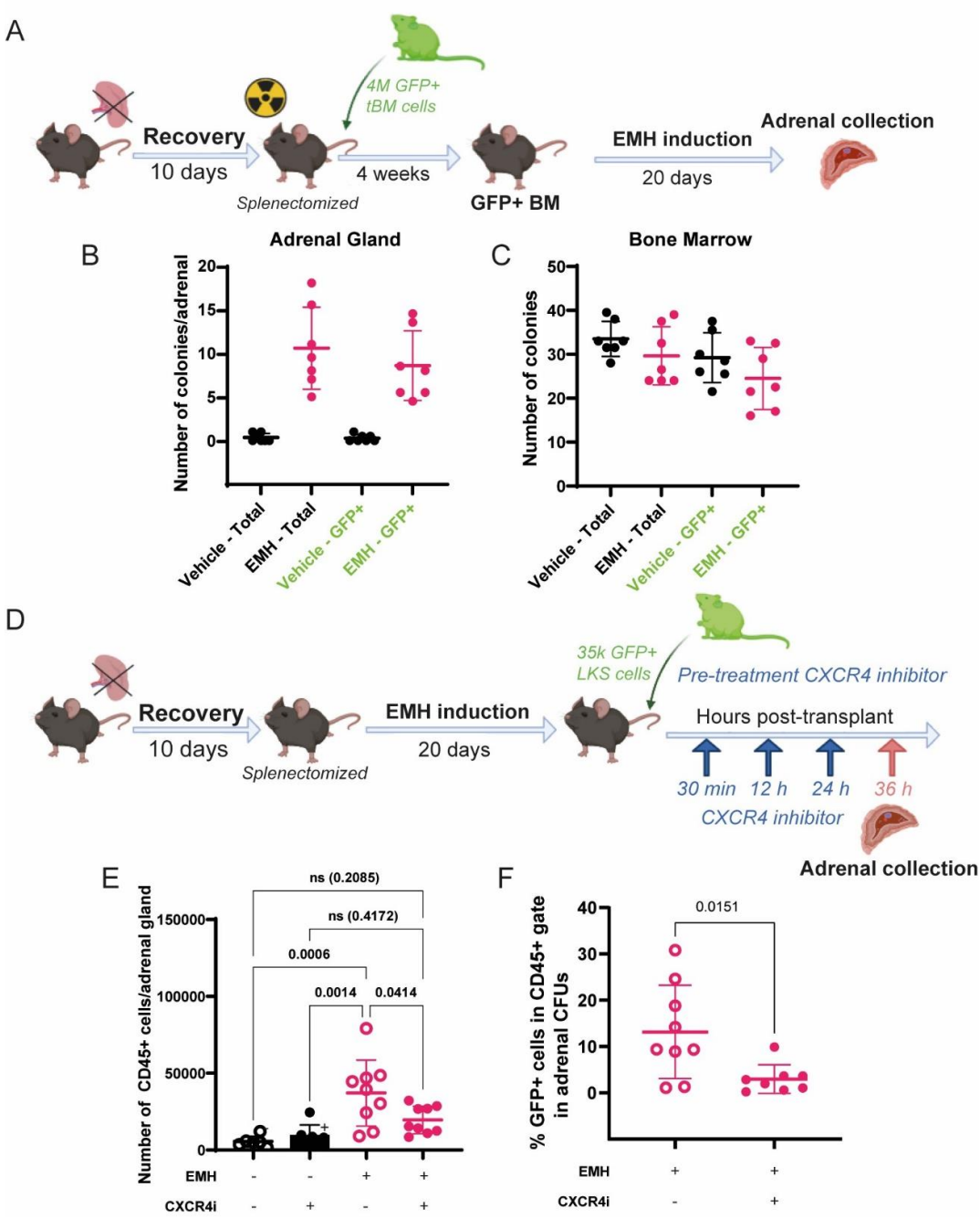

Figure 3. The adrenal stroma recruits and supports circulating hematopoietic progenitors

A Experimental design for EMH induction after transplant with GFP+ BM. **B, C** CFU assay, number of total colonies and GFP+ colonies per single adrenal gland (**B**) and 10,000 CD45+ total bone marrow cells (**C**) (n=6 per experimental group, two independent experiments). **D** General experimental design for homing assay. **E** CD45+ cells in EMH-induced adrenals glands retrieved from mice treated with plerixafor (CXCR4i), evaluated by flow cytometry (two independent experiments, n=8 for control groups and n=10 for EMH-induced groups). **F** Percentage of GFP+ cells from the recovered cells grown in methylcellulose CFU culture after completion of the CFU assay (8 days post-plating), quantified by flow cytometry (n=9 control mice and n=8 experimental mice). Data are represented as mean ±SD and groups were compared with one-way ANOVA followed by Tukey's multiple correction test (**E**) or two-tailed, unpaired Student's *t*-test (**F**).

Figure 4

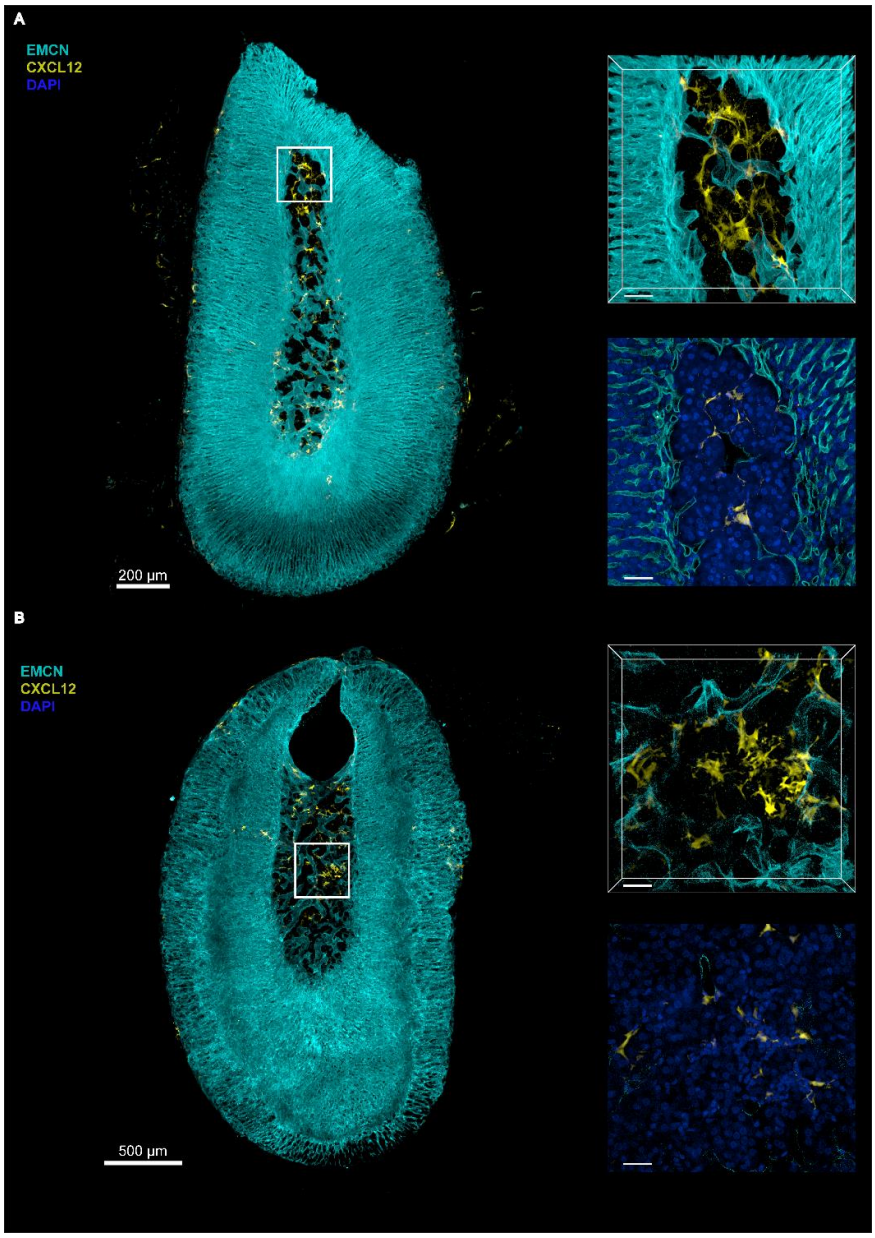

Figure 4. The murine adrenal gland contains CXCL12-positive cells

3D Microscopy of murine adrenal glands: Representative 3D sections and optical slices of immunostained adrenal glands from (A) control-treated (n=3) and (B) EMH-induced (n=3) Cxcl12^{GFP} transgenic mice showing Endomucin (EMCN;Cyan), CXCL12-GFP (yellow) and 4′,6-diamidino-2-phenylindole (DAPI;blue). Scalebars (A) 200 µm, (B) 500 µm; for all cropped sections and optical slices scalebars represent 40 µm.

Figure 5

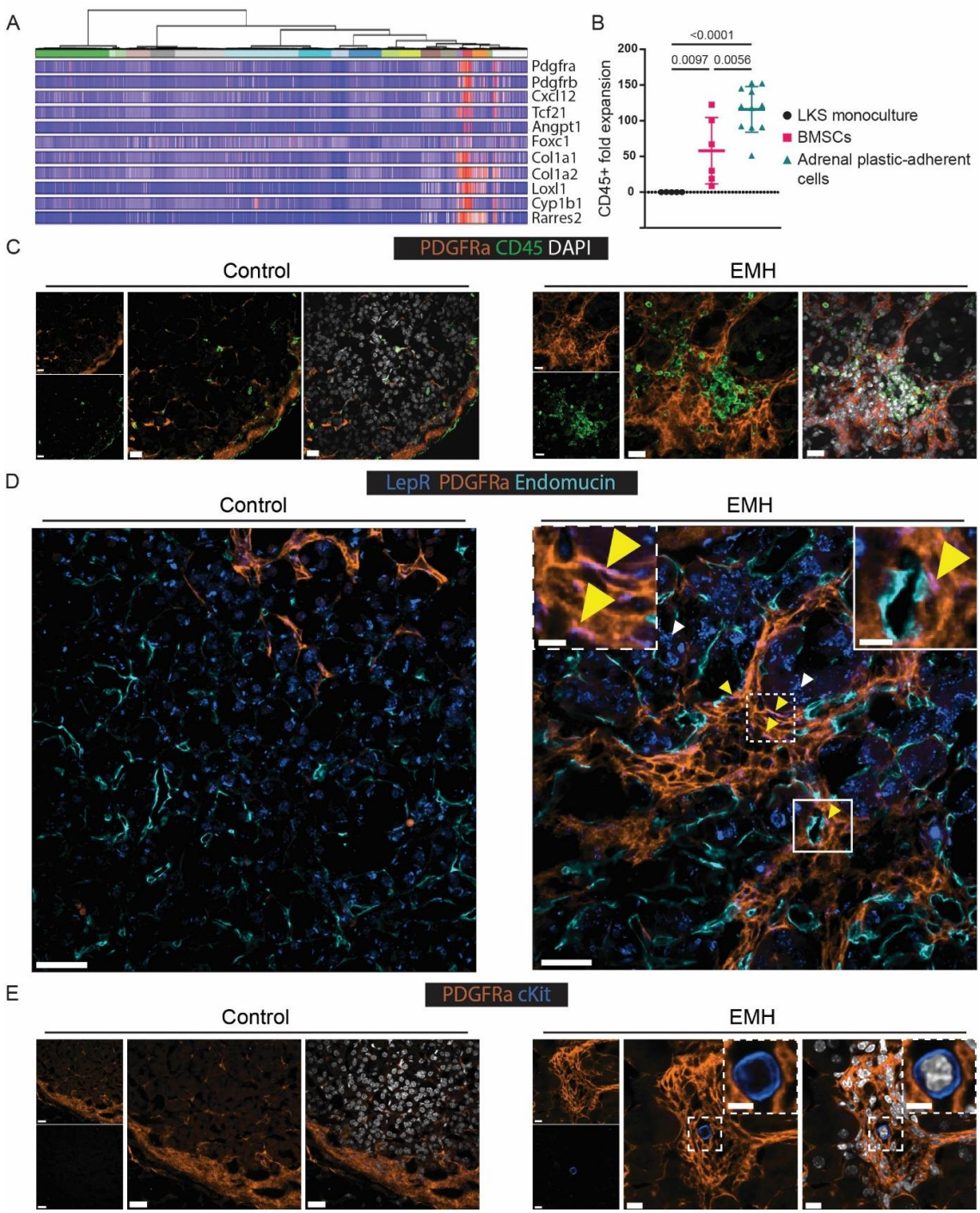

Figure 5. EMH-induced adrenal glands have a modified stromal architecture with PDGFRa clusters hosting hematopoietic foci with rare c-kit+ HSPCs.

A, Selection of genes enriched in the PDGFRa-expressing cells of the murine adrenal gland (PDGFRa-expressing clusters: mC6 "mesenchymal" in red and mC13 "capsule" in purple, as defined by Bedoya-Reina et al. 2021). **B**, Adrenal plastic-adherent cells are supportive of CD45+ cell expansion. Expansion of total hematpoietic cells (CD45+) upon coculture for 7 days of FACS-sorted murine HSPCs (LKS) with a confluent feeder layer of BMSCs obtained from flushed, collagenase-digested bones or adrenal gland, in the absence of additional cytokines. Data are represented as mean ±SD and groups were compared with one-way ANOVA followed by Holms-Sidak multiple correction test (n=5 for LKS monoculture, 6 for BMSCs and 11 for

adrenal plastic-adherent cells. Data were obtained in 2 independent experiments). **C**, Representative images of control and EMH-induced adrenal glands (n=2-3 mice per group) stained for CD45 (green), PDGFRa (orange) and DAPI (white). Scale bars represent 20 µm in all instances in C. D**,** Representative images of control and EMH-induced adrenal glands (n=2, multiple nodules per adrenal) stained for LepR (blue), PDGFRa (orange), endomucin (teal). Yellow arrowheads indicate examples of colocalization of PDGFRa and LepR (co-localization in pink), where the latter has an elongated pattern marking cells in pericyte position, while white arrowheads indicate adrenal parenchyma cells that display a different pattern of LepR, mostly perinuclear. Scale bars represent 20 µm in all instances in **D** except for the inset, in which it represents 5 µm. **E,** Representative images of control and EMH-induced adrenal glands (n=3, multiple nodules per adrenal) stained for PDGFRa (orange), cKit (blue), and DAPI (white). Scale bars represent 20 µm in the controls, 10 µm in the EMH-induced mice. The scale bar in the inset represents 5 µm.

Figure 6

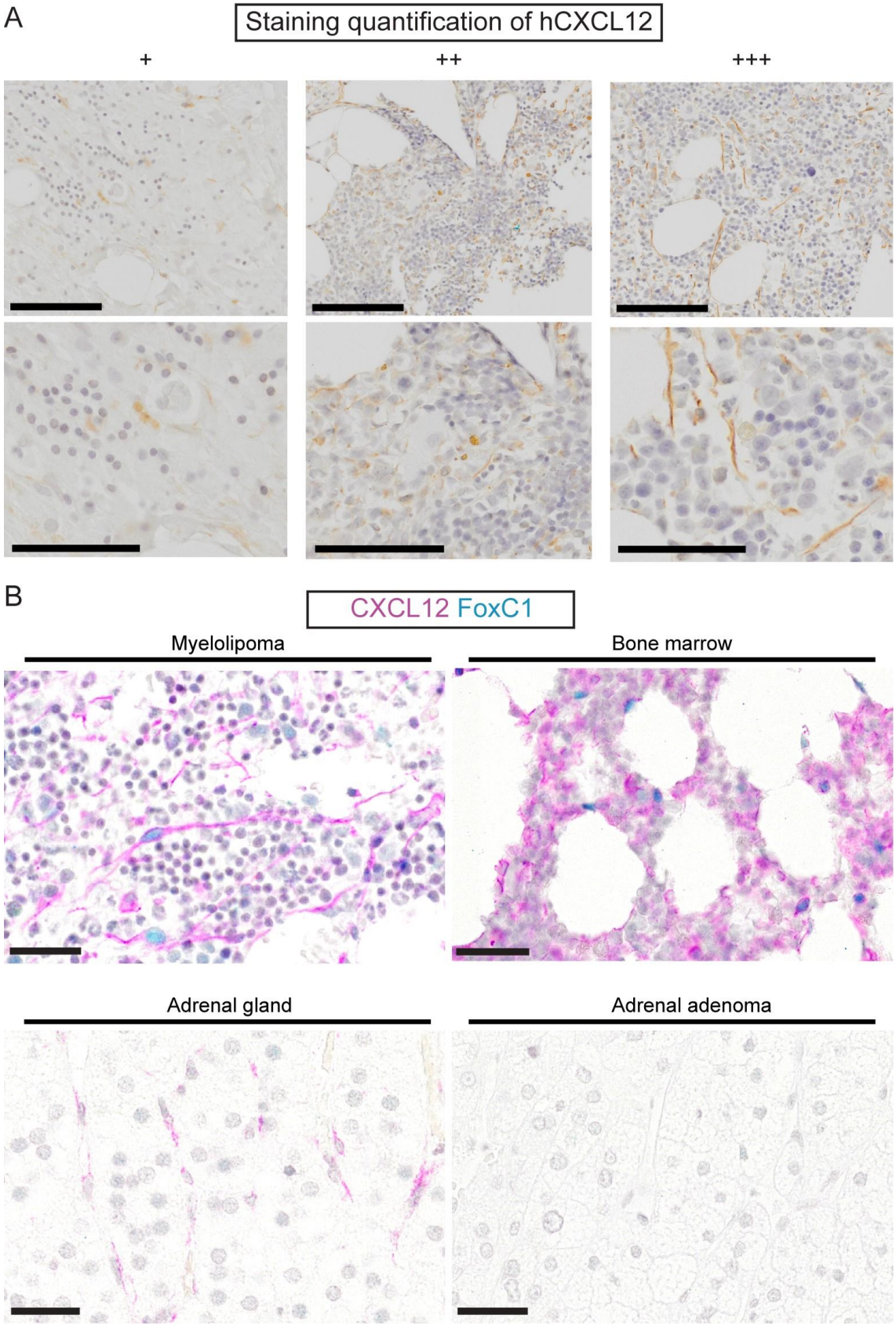

Figure 6

Figure 6. CXCL12+ cells of stromal morphology are present in human myelolipoma and co-express FoxC1.

A. Representative images of CXCL12 IHC stains of human myelolipoma samples corresponding, from left to right, to patients I, C and D (see Table 1 for details). Scale bars correspond to 200 µm and 100 µm in the left and right columns, respectively. **B**. Double chromogenic immunohistochemical stain for CXCL12 (pink) and FoxC1 (teal) in human myelolipoma, bone marrow, healthy adrenal gland, and adrenal adenoma. Scale bar represents 30 µm in all instances.